Single-file mobility of water-like fluid in a generalized Frenkel-Kontorova model

Patricia Ternes, Alejandro Mendoza-Coto, and Evy Salcedo

Citation: The Journal of Chemical Physics **147**, 034510 (2017); doi: 10.1063/1.4995448
View online: http://dx.doi.org/10.1063/1.4995448
View Table of Contents: http://aip.scitation.org/toc/jcp/147/3
Published by the American Institute of Physics

Single-file mobility of water-like fluid in a generalized Frenkel-Kontorova model

Patricia Ternes,[1,a)] Alejandro Mendoza-Coto,[2,b)] and Evy Salcedo[3,c)]
[1]*Instituto de Física, Universidade Federal do Rio Grande do Sul, Caixa Postal 15051, 91501-970 Porto Alegre, RS, Brazil*
[2]*Departamento de Física, Universidade Federal de Santa Catarina, 88040-900 Florianópolis, Santa Catarina, Brazil*
[3]*Coordenadoria Especial de Física, Química e Matemática, Universidade Federal de Santa Catarina, Rua Pedro João Pereira, 150, 88905-120 Araranguá, SC, Brazil*

(Received 10 May 2017; accepted 11 July 2017; published online 21 July 2017)

In this work, we used a generalized Frenkel-Kontorova model to study the mobility of water molecules inside carbon nanotubes with small radius at low temperatures. Our simulations show that the mobility of confined water decreases monotonically increasing the amplitude of the substrate potential at fixed commensurations. On the other hand, the mobility of the water molecules shows a non-monotonic behavior when varying the commensuration. This result indicates that the mobility of the confined fluid presents different behavior regimes depending on the amplitude of the water–nanotube interaction. In order to qualitatively understand these results, we study analytically the driven Frenkel-Kontorova model at finite temperatures. This analysis allows us to obtain the curves of the mobility versus commensurations, at fixed substrate potentials. Such curves show the existence of three regimes of mobility behavior as a function of the commensuration ratio. Additionally, our study indicates a nontrivial and strong dependence of the mobility with a quantity that can be interpreted as an effective amplitude of the substrate potential, depending on the bare amplitude of the substrate potential, the commensuration ratio, and temperature. *Published by AIP Publishing.* [http://dx.doi.org/10.1063/1.4995448]

I. INTRODUCTION

A fluid in nanoscale confinement can present a dramatic change in its properties when compared with its bulk behavior. This occurs mainly due to the confining surface that, in this scale, is structured and smooth.

Single-wall carbon nanotubes (CNTs) have a periodic structure[1] which allows the confined fluid to present anomalous behavior.[2,3] Moreover, they present excellent electronic and mechanical properties, which makes them a promising nanochannel for a variety of applications in nanotechnology, specially in the biotechnology field.[4–9] Therefore, the behavior of water confined inside CNTs has been extensively studied. These studies showed that, under confinement, water presents an anomalous flow when compared with predictions of classical hydrodynamic theory.[10–17]

However, this anomalous behavior is not entirely understood. Experimental results showed that the water flow enhancement factor can vary from one to three orders of magnitude,[10–12] while simulation studies show an enhancement of up to five orders of magnitude.[13–16] Beyond the range issue of results, there is no consensus about the enhancement factor behavior. Some previous studies present a monotonic enhancement with decreasing radius,[10,15] while others present a discontinuous enhancement factor.[12,16] A simple explanation to the water mobility behavior was proposed by Falk *et al.*[18] They found that the nanotube curvature, given by the inverse of the nanotube radius, has a strong effect on the water-CNT commensuration ratio: for more curved nanotubes, she found more misfits for water molecules over the internal nanotube surface, leading to a higher mobility, while for a flat surface (in slab geometry), the mobility is independent of confinement (slab separation). So, for Falk *et al.*, the high mobility is mainly related to the curvature-induced water–carbon incommensurability.[18]

Water has a complex phase diagram and there is no model to describe its behavior entirely. Several atomistic models were proposed in order to describe water's behavior, usually at ambient pressure and temperature.[19,20] Besides these models, effective models have been widely employed in order to study anomalous behavior in bulk water-like systems.[21–25] In these effective models, it is considered that bulk water form small clusters of four water molecules and that these clusters come together to form water bicyclo-octamers of different densities. However, in confined systems, these structures are completely different and heavily dependent on the tube geometry and water model employed.[2,12,26–28] For CNTs with radius sufficiently small, the confined water molecules form single-file chains, an arrangement that is an almost one-dimensional and highly oriented hydrogen-bonded network. Therefore, the choice of the inter-particle water potential is not trivial.

Understanding the water flow inside CNTs is a very complex task because the current available technology has a limited capacity to directly "look" at the dynamics of the confined molecules.[29,30] So, to model the water-CNT system, theoreticians need to have some insight into a known nanoscopic

[a)]Electronic mail: patricia.terdal@gmail.com
[b)]Electronic mail: alejandro.mendoza@ufsc.br
[c)]Electronic mail: evy.salcedo.torres@ufsc.br

system, for example, the dynamics of atoms or molecules on a surface. To study the nanoscale friction, several experimental methods have been developed to measure directly or indirectly the mobility of atoms or molecules on a surface. In this context, it is preferable to talk in terms of friction and mobility, rather than flow.

The most prominent apparatus developed to study the nanoscale friction was the atomic force microscope (AFM). AFM studies show that on the nanoscale the same physical system can exhibit dry friction (like solid–solid friction) or wet friction (like liquid–solid friction), depending on several factors such as module of shear stress, applied time of shear stress, etc.[31–33] This behavior is completely different from that observed for a macroscopic or even mesoscopic system. Through the quartz crystal microbalance (QCM), a novel experimental method developed by Krim, it was observed systematically that wet friction can indeed occur in structured systems.[34–36] The results of QCM introduce a new key question to be answered: What is the main way of dissipation of energy in the nanoscale wet friction: the internal excitation due the interactions with the surface topology (phononic friction)[37–40] or the process of excitation of low-energy electron-hole pairs on the surface (electronic friction)?[41–46] To answer this question, several and beautiful arrangements were developed (from experimental perspective); even systems on a superconducting state were analyzed.[36,47] From theoretical perspective, almost all studies were addressed by molecular dynamics simulation using a generalized Frenkel-Kontorova (FK) model as a paradigm.[37–39,48,49]

Our aim in this work is to study the relation between the confined water mobility and the CNT topology. To do this, we performed molecular dynamics simulations using a generalized Frenkel-Kontorova model. The potentials were chosen to effectively reproduce the water behavior when confined in carbon nanotubes with very small radius (single-file state). The effect of the nanotube can be illustrated by a naïve analogy with an egg carton, the energy landscape being smoother for nanotubes with smaller radius,[18] and the behavior of single-file water can be approximated as a one-dimensional chain of particles interacting through a two length scale isotropic potential. To capture the topological effects on water mobility using the FK model, simulations should be performed in the low temperature regime. To avoid water freezing, perfect commensuration ratios (0.5, 1.0) were avoided as well. Additionally, using an analytical analysis, we found a relation between the mobility's behavior as a function of temperature (as predicted phenomenologically[50,51]) and corrugation. This paper is organized as follows: in Sec. II we present the generalized Frenkel-Kontorova model used in the characterization of the mobility of a confined water-like fluid. In Sec. III we present and discuss the simulation results. To continue, Sec. IV shows an analytical analysis of the FK model at finite temperatures. Finally, in Sec. V our conclusions are presented.

II. A GENERALIZED FRENKEL-KONTOROVA MODEL

In this section, we present the model used to study the dynamics of water molecules in a single-file structure flowing inside a carbon nanotube. Our system of particles is studied by means of a one-dimensional generalized Frenkel-Kontorova model. In this way, the single-file structure is regarded as a chain of particles with mass m, interacting through a core-softened potential $V(x_{ij})$ [Eq. (2)], where $x_{ij} = x_i - x_j$ represents the distance between particles i and j. Moreover we modeled the influence of the structured nanotube by the presence of an external periodic potential, $U(x_i)$ [Eq. (3)]. To induce a net flow of particles in a given direction, we applied an external force F on each particle of the system.

Additionally, the temperature is fixed by adding a stochastic force, $f_i(t)$, and a viscous damping force, $-m\eta_{ad}\dot{x}_i$. The stochastic force is related to the temperature and with the *ad hoc* damping constant (η_{ad}) by means of the fluctuation-dissipation theorem: $\langle f_i(t) f_j(0)\rangle = 2\eta_{ad} m k_B T \delta_{ij}\delta(t)$. Here k_B is the Boltzmann constant and η_{ad} can be thought as a result of the influence of certain degrees of freedom inherent of real physical systems that are not included in our model. With such ingredients, the equation of motion of our system is given by the following Langevin equation:

$$m\ddot{x}_i(t) + \eta_{ad}\dot{x}_i(t) = -\frac{dU(x_i)}{dx_i} - \frac{dV(x_{ij})}{dx_i} + f_i(t) + F_i. \quad (1)$$

The interaction between particles, $V(x_{ij})$, is a potential obtained by the addition of 3 different Fermi–Dirac distributions,[52]

$$V\left(x_{ij}\right) = \sum_{k=1}^{3} \frac{\varepsilon_k}{\exp\left(\frac{x_{ij}-r_{0k}}{\sigma_k}\right) + \alpha_k}, \quad (2)$$

where $x_{ij} = |x_j - x_i|$ is the distance between two water-like particles. Table I shows the parameters used for $V(x_{ij})$ in our simulations. The periodic potential $U(x_i)$ representing the water-CNT interaction is

$$U(x_i) = u_0 \cos\left(\frac{2\pi}{a} x_i\right), \quad (3)$$

a and u_0 being the periodicity and the amplitude of the potential, respectively. The amplitude of potential is also called corrugation. We choose the parameters for the potentials $V(x_{ij})$ and $U(x_i)$ to effectively reproduce the water–water and water–CNT interactions for the TIP3P water model confined in a nanotube. The complete discussion for these potential determinations can be found in the supplementary material.

In what follows, we take the equilibrium distance between two oxygens of molecules forming a hydrogen bond as r_I, the energy of the hydrogen bond as E_I, and the mass m of a water molecule as the fundamental units of the problem. Consequently all physical quantities are expressed in reduced

TABLE I. Parameters for the potential $V(x_{ij})$ in reduced units of m, E_I, and r_I.

$\varepsilon^*_{1,2,3}$	1.0	−0.001	−0.999
$r^*_{0_{1,2,3}}$	0.940	1.025	1.105
$\sigma^*_{1,2,3}$	0.005	0.005	0.005
$\alpha_{1,2,3}$	0.0	1.0	1.0

units as

$$x^* \equiv x r_I^{-1}, \qquad F^* \equiv F r_I E_I^{-1},$$
$$T^* \equiv T k_B E_I^{-1}, \qquad t_0 \equiv r_I (m/E_I)^{1/2},$$
$$V^* \equiv V E_I^{-1}, \qquad t^* \equiv t t_0^{-1},$$

where t is time.

The length of the chain of particles is fixed; consequently in order to impose periodic boundary conditions, we have the following constraint: $Ma = Nr_I$, where a was defined in Eq. (3), N corresponds to the number of particles in our chain, and M represents the number of minimums of the potential within the chain. Now we define the so-called commensuration ratio as

$$\zeta = \frac{a}{r_I} = \frac{N}{M}. \tag{4}$$

Since E_I and r_I were taken as fundamental units, changes in the structure of confined water are reflected in a commensuration variation while little changes in the CNT geometry are treated through a corrugation variation.[18] Therefore, u_0 and ζ are our key parameters in the mobility study of the chain particles.

Equation (1) is numerically integrated using a Brownian molecular dynamics algorithm,[53] for $N = 4096$ particles with a time step $dt = 0.001t_0$ at $T^* = 0.05$. We allow the system to relax during a time interval of $2000t_0$, in the sequence an external force $F^* = 0.0003$ is applied; after another transient period of order $6000t_0$, the system reaches the steady state and the external force is turned off making the velocity of particles decay back to zero. Figure 1 shows the typical behavior of the center-of-mass velocity of the chained particles during simulation.

The autocorrelation function of the velocities between several different samples, in the decay region (after the driving force is turned off), has the following exponential form:[54]

$$\gamma(t - t') = \exp\left(-\eta |t - t'|\right), \tag{5}$$

where η will be the effective microscopic friction coefficient. An exponential decay of the velocity autocorrelation function as the one given by Eq. (5) is a characteristic of the fluid on solid systems.[55] We expect the measured η to be higher than the *ad hoc* damping constant (η_{ad}), which was set to $5 \times 10^{-3} t_0^{-1}$. Finally all simulations were carried out at fixed temperature, volume, and number of particles.

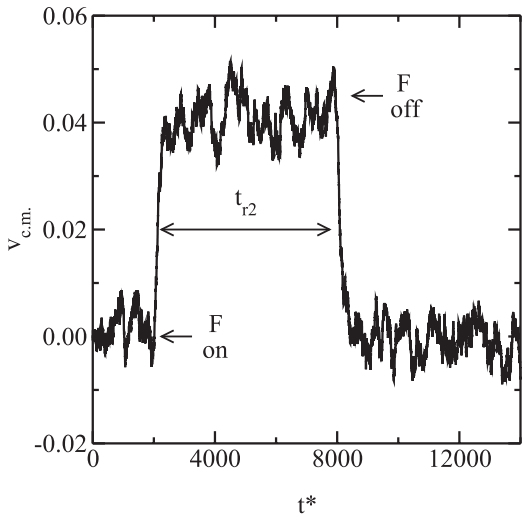

FIG. 1. Typical behavior of the center-of-mass velocity of the chain particles versus time. In this case, $\zeta = 0.68$ and $u_0^* = 0.04$.

III. COMPUTATIONAL RESULTS

We carried out simulations with several commensuration ratios between 0.55 and 0.91 and corrugation values from 0.01 to 0.10. For all these parameters, wet friction was observed. In all cases, the coefficient of friction was obtained from fits according to Eq. (5). To calculate the velocity autocorrelation function, we used fifty different samples of the velocity relaxation.

Figure 2 shows the total friction coefficient as a function of corrugation for some commensuration ratios. These results show that as the corrugation increases, the friction experienced by the water-like particles increases. An analysis of the curves $\eta \times u_0$ shows that these curves present a power law behavior given by

$$\eta = \eta_0 + c u_0^n. \tag{6}$$

Furthermore in the limit of corrugation going to zero ($u_0 \to 0$), the coefficient η_0 has an average value equal to the *ad hoc* damping constant: $\eta_0 = 0.005 \pm 0.001$. Therefore, it is natural to assume that the topological influence in the mobility is represented by the second term of Eq. (6): cu_0^n, where the average value of n obtained from the best fit is equal to 1.9 ± 0.3. It is worth noticing that a number of previous analytical and numerical studies report a quadratic behavior of friction with corrugation amplitude: for a fluid on a surface,[37,38,48,49] for a fluid slab confined between parallel solid walls,[56] and for TIP3P water confined in carbon nanotubes.[18]

The central quantity in our study is the mobility, B, of the particle chain, which is defined as the inverse of the friction coefficient η: $B = \eta^{-1}$. In Fig. 3 we showed the normalized mobility as a function of the commensuration ratios. The mobility decreases as the corrugation increases for all studied

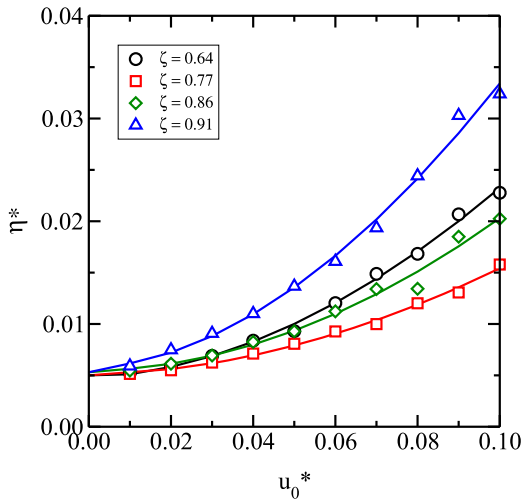

FIG. 2. Total friction coefficient for some commensurations ζ: black circles 0.64, red squares 0.77, green diamonds 0.86, and blue up triangles 0.91. The solid lines are fits to Eq. (6). Error bars are omitted because they are smaller than the size of the symbols.

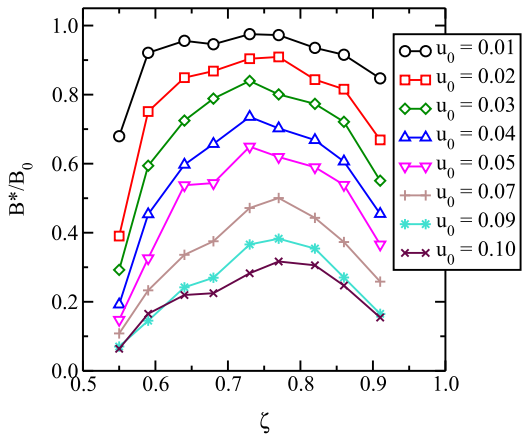

FIG. 3. Normalized mobility as a function of commensuration ratios for some substrate potential amplitude u_0^*, where B_0 is the mobility in the limit of absence of corrugation ($u_0 \to 0$). Error bars are omitted because they are smaller than the size of the symbols.

corrugation amplitudes, but the relation between commensuration and mobility is non-monotonic. The mobility as expected does have a local minimum for commensuration ratios close to 1/2 and 1. For commensuration ratios between these values, the mobility increases reaching a local maximum value in a region close to $\zeta = 3/4$. In addition, for corrugations higher than $u_0 = 0.05$, the mobility presents a change of curvature at ζ close to 2/3. These results indicate the existence of different mobility regimes depending on the amplitude of interaction between the water-like particles and CNT surface.

At this point, it is interesting to take into consideration the work of Braun and Kivshar,[50] which studied the behavior of the mobility as a function of temperature and commensurations, at fixed corrugation for the Frenkel-Kontorova model. Although our results for the mobility were obtained for a different model and varying corrugation and commensuration at fixed low temperature, we will show shortly that there is a close relation between our results and those of Braun and Kivshar.[50]

In that work, the authors present a phenomenological approach that describes the transport properties in terms of moving defects (kinks) in the density of particles along the chain. Kinks describe local expansions or compressions of the chain which are at the core of the mechanism producing mass transportation. It is expected that the higher the concentration of kinks, the greater the mobility. According to Ref. 50, at high temperatures the concentration of kinks produced due to thermal fluctuations has a maximum at $\zeta = 3/4$, and consequently the mobility has a local maximum in this region.

For lower temperatures, the concentration of kinks depends on the degree of frustration in the system's geometry. When the mean distance between particles coincides with the distance between two minima of the external periodic potential ($\zeta = 1/2$ and 1), the system is in a commensurate ground state and particles are pined. For commensurations between these values, there is a nonzero probability to find particles close to the maximum of the external potential which increases the kinks' concentration. This produces an increment in the particle mobility. For commensuration equal to the golden mean $\zeta = 2/(1+\sqrt{(}5))$, the geometric frustration is maximal as well as the kinks' concentration; therefore, a local maximum in the mobility occurs. However, in these conditions, for sufficiently low temperatures due to the high density of kinks, a regular lattice of kinks is formed, decreasing the mobility strongly. This behavior is observed first for commensurations close to the golden mean. From this state, a further decrease of temperature produces similar falls in mobility for commensurations such as 3/4, 3/5, or 4/5.[51]

As we mentioned before, this phenomenological description is directly related to changes in temperature. However our computational results were obtained keeping the temperature fixed at a low value while the corrugation was varied. Even so, some similarities arise. Figure 3 presents two important results. First, the mobility depends on the commensuration ratio as described by Braun and Kivshar.[50,51] Second, the mobility presents different regimes depending on the substrate amplitude. From the theoretical background at nanoscale friction, we have different mobility regimes due to the activation of geometric or thermal kinks, depending on the system temperature The similarities between the Braun and Kivshar results for the mobility at constant corrugation varying temperature[50] and ours obtained varying corrugation at fixed temperatures motivate us to pursue further investigation of the corrugation versus temperature interplay. The main objective of this investigation is to provide an explanation for the existence of different mobility regimes as a function of corrugation observed in Fig. 3.

IV. THEORETICAL DISCUSSION

In order to explain the previously obtained results for the mobility, in both the classic and in our generalized Frenkel-Kontorova models, we decided to study analytically the behavior of the mobility in the classic FK model at finite temperatures. We begin considering the following equation of motion for the system of interacting particles:

$$m\ddot{x}_i + \eta\dot{x}_i = K(x_{i-1} + x_{i+1} - 2x_i) - \frac{dU}{dx}(x_i) + F + f_i(t), \quad (7)$$

where $U(x)$ represents the substrate potential taken as $U(x) = -u_0\cos(k_0 x)$. Choosing now $l_0 = k_0^{-1}$ and $\sqrt{m/K}$, as units of length and time, respectively, we can rewrite our system of equations in terms only of dimensionless variables,

$$\ddot{r}_i + \tilde{\eta}\dot{r}_i = (r_{i-1} + r_{i+1} - 2r_i) - g\sin(r_i) + \tilde{F} + \tilde{f}_i(\tilde{t}), \quad (8)$$

where r and $\tilde{t}$ represent the dimensionless position and time, while $\tilde{\eta} = \eta/\sqrt{mK}$, $g = u_0 k_0^2/K$, $\tilde{F} = k_0 F/K$, and $\tilde{f}_i(\tilde{t}) = k_0 f_i(t)/K$. In what follows, we will omit tildes in dimensionless quantities to simplify the notation.

In order to calculate analytically the stationary mobility of the system, defined as the ratio of the driving force divided by the average stationary velocity of the particles, we need to determine the stationary state of the system described by Eq. (8). A procedure to find such a stationary state has been developed in Ref. 57. Nevertheless such a technique cannot be applied directly in our case due to the presence of the thermal noise. However, if we perform an average over thermal noise realizations in each term of Eq. (8), we will recover a deterministic equation for which techniques developed by Strunz

and Elmer[57] can be applied. By performing such average, we reach

$$\langle \ddot{r}_i \rangle + \eta \langle \dot{r}_i \rangle = (\langle r_{i-1} \rangle + \langle r_{i+1} \rangle - 2\langle r_i \rangle) - g\langle \sin(r_i) \rangle + F. \quad (9)$$

To proceed, we need to calculate the thermal average of $\sin(r_i)$. This term can be evaluated by using the following mean field argument: first we consider that the stationary sliding state is uniform, and in this sense, it means that within the mean field approximation, we could use a single particle Fokker–Planck equation to study the dynamics of a single particle density and conclude that within such approximation the average time dependent single particle probability distribution will be

$$P(x,t) = \sqrt{\frac{K}{\pi k_B T}} \exp\left(-\frac{k(x-vt)^2}{k_B T}\right). \quad (10)$$

To reach such a result, it is implicit that in thermal equilibrium the average distance between particles is equal to the equilibrium distance between them in the absence of all external forces. With Eq. (10) in mind, we can conclude that

$$\langle \sin(r_i(t)) \rangle = \sin(\langle r_i(t) \rangle) \exp\left(-\frac{k_0^2 k_B T}{4K}\right). \quad (11)$$

This relation implies that Eq. (9) can be written as

$$\langle \ddot{r}_i \rangle + \eta \langle \dot{r}_i \rangle = (\langle r_{i-1} \rangle + \langle r_{i+1} \rangle - 2\langle r_i \rangle) - g_r \sin(\langle r_i \rangle) + F, \quad (12)$$

where $g_r = g \exp\left(-\frac{k_0^2 k_B T}{4K}\right)$. Interestingly these results imply that the dynamics of the driven Frenkel-Kontorova model at finite temperatures is equivalent to the one at zero temperature, with a modified effective potential substrate amplitude. Now we can directly apply the techniques developed by Strunz and Elmer[57] to study the stationary uniform sliding state of Eq. (12).

The aforementioned method proposes an ansatz for the stationary form of the position of the particles as a function of time. The proposed functionality is given by

$$r_i = \psi + ai + vt + f(\psi + ai + vt), \quad (13)$$

where ψ represents an arbitrary phase, $a = k_0 l$ is the equilibrium distance between particles in units of k_0^{-1}, and v corresponds to the stationary velocity of the system of particles. Moreover the function $f(x)$ is the so-called hull function, which is a zero mean periodic function characterizing the oscillation of the particle over its uniform translational movement due to the presence of the periodic potential.

To continue, we substitute the previous ansatz for $r_i(t)$ into our equation of motion [Eq. (12)]. This procedure leads us to the following differential equation for the hull function:

$$v^2 f''(\phi) + \eta v(1 + f'(\phi)) = (f(\phi - a) + f(\phi + a) - 2f(\phi)) - g\sin(\phi + f(\phi)) + F. \quad (14)$$

Considering now that $f(\phi)$ must be a periodic function with zero mean, we know that we can write the hull function as $f(\phi) = \sum_{n=1}^{\infty} a_n \cos(n\phi) + b_n \sin(n\phi)$, where a_n and b_n represent the Fourier expansion coefficients of the hull function. If the Fourier expansion for $f(\phi)$ is substituted in Eq. (14), we can reach the following system of equation for the Fourier coefficients:

$$\begin{aligned} &\left[v^2 n^2 + 2(\cos(na) - 1)\right] a_n - \eta v n b_n \\ &\quad = g \int_0^{2\pi} \frac{d\phi}{\pi} \sin(\phi + f(\phi)) \cos(n\phi), \\ &\left[v^2 n^2 + 2(\cos(na) - 1)\right] b_n + \eta v n b_n \\ &\quad = g \int_0^{2\pi} \frac{d\phi}{\pi} \sin(\phi + f(\phi)) \sin(n\phi). \end{aligned} \quad (15)$$

Once the Fourier coefficients have been determined, the driving force F can be calculated in terms of v and the set of Fourier coefficients a_n, b_n. This relation can be proven to be[57]

$$F = \eta v \left(1 + \frac{1}{2} \sum_{n=1}^{\infty} n^2 (a_n^2 + b_n^2)\right). \quad (16)$$

Considering that the method outlined allows us to calculate the values of stationary velocity v for a given driving force F, we can now calculate the mobility of the system. The computational study presented focused on the role of the commensuration in the behavior of the mobility at different amplitudes of the substrate potential. Now we will determine similar curves numerically for the Frenkel-Kontorova model for comparison with the computational results from simulations.

To continue, we need to write all our dimensionless parameters in terms of the commensuration parameter ζ defined as $2\pi/a$ and an appropriate energy scale; such an energy scale is chosen as Kl.[2] This leads us to the following relations:

$$\begin{aligned} g &= u_0 \frac{4\pi^2}{\zeta^2} \exp\left(-\frac{\pi^2}{\zeta^2}\tilde{T}\right), \\ F &= \frac{2\pi}{\zeta}\tilde{F}, \\ a &= \frac{2\pi}{\zeta}, \end{aligned} \quad (17)$$

where $u_0 = u/(Kl^2)$, $\tilde{T} = (k_B T)/(Kl^2)$, and $\tilde{F} = F/(Kl)$. To conclude, we set $\eta = 1$ and proceed with the numerical study.

The first thing that is worth noticing is the nontrivial dependence of the effective lattice potential g in terms of the commensuration ζ. As we can observe from Fig. 4, the effective potential to which particles are submitted in general varies strongly with the commensuration and at the same time such variation depends critically on temperature. More important than this is to note from Eqs. (17) that the effective corrugation g depends on both the bare corrugation and the temperature. In fact at fixed commensuration, the effective corrugation is an increasing monotonic function of u_0 and a decreasing monotonic function of temperature. Equations (17) clarify the interplay between temperature and substrate potential and ultimately allow us to establish a connection between the behavior of the mobility, varying corrugation at fixed temperature and varying temperature at fixed corrugation. To explore the consequences of our analytical calculations, we proceed with the calculus of the mobility curves varying the corrugation at fixed temperatures.

Now we can describe the protocol followed for the numerical solution of Eq. (15). As input parameters, we have the

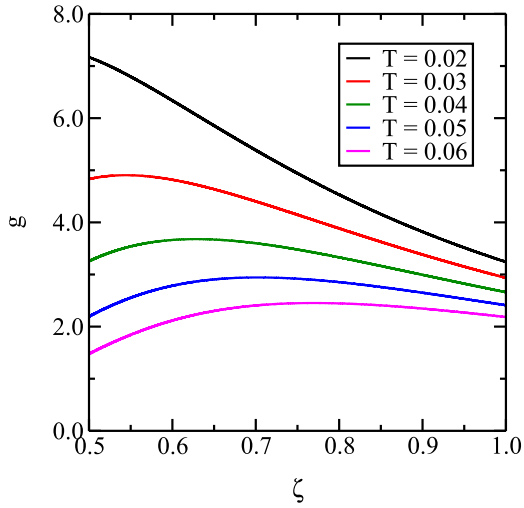

FIG. 4. Effective substrate amplitude potential as a function of the commensuration at different temperatures for $u_0 = 0.1$. As shown in the figure, the effective substrate potential as a function of *xi* depends critically on temperature.

friction coefficient η, set to one, the geometrical parameter a, the effective corrugation potential g, and the stationary mean velocity v. With the numerical solution at hand, the calculation of the driving force F producing such stationary velocity can be carried out by directly applying Eq. (16). This procedure is used to calculate the normalized mobility defined as $B = (\eta v)/F$ following Eq. (16). As can be noticed from this equation, the normalized mobility is always a quantity lower than one, being one only in the limit of zero corrugation potential.

We proceed next with the construction of families of normalized mobility curves varying commensuration, for various amplitudes of the corrugation potential at fixed temperature and driving force. We construct these families for two relatively low temperatures arbitrarily chosen: $\tilde{T}_1 = 0.038$ (Fig. 5) and $\tilde{T}_2 = 0.05$ (Fig. 6). At the same time, the bare corrugation potential u_0 was let to range from 0.01 to 0.1 and the driving force in all cases was taken as 0.13. It is worth noticing that although all numerical values were selected arbitrarily,

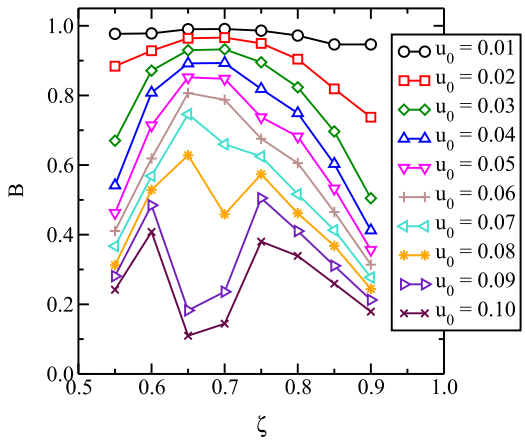

FIG. 5. Normalized mobility at $\tilde{T} = 0.038$ for different amplitudes of the substrate potential u_0. All curves were calculated at a fixed driven force $\tilde{F} = 0.13$.

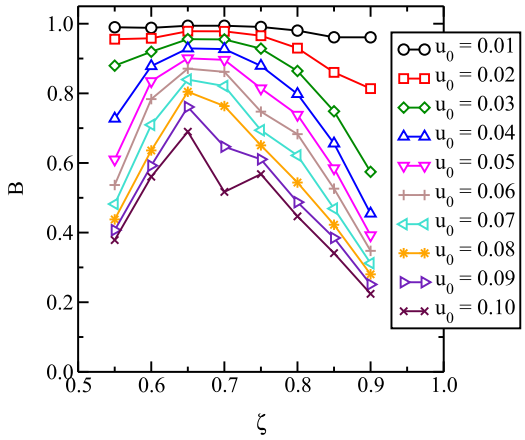

FIG. 6. Normalized mobility at $\tilde{T} = 0.05$ for different amplitudes of the substrate potential u_0. All curves were calculated at a fixed driven force $\tilde{F} = 0.13$.

since the values of the temperature strongly affects the effective value of the substrate potential, much higher temperatures will result in very small g leading the system to a trivial regime out of the scope of the present work.

In Figs. 5 and 6, a number of regularities appear, as a reflection of a robust physics over variations of temperature and substrate potential. To qualitatively understand the behavior of the mobility, we make use of the picture given by Braun *et al.*[50,51] previously discussed in Sec. III. First it is important to notice that the maximum of the mobility should be reached when the concentration of kinks is maximum as well. As we know, there are two sources of kinks: those produced by the geometric frustration and those due to thermal fluctuations. According to Braun *et al.*[50,51] in the high temperature regime, or equivalently in the low substrate potential regime (as discussed previously), we have a maximum of the total number of kinks at commensurations around $\zeta = 3/4$, reflecting in a maximum of the mobility at such commensurations, as observed in Figs. 5 and 6.

Lowering temperatures, or increasing u_0, the population of thermally activated kinks decreases considerably making geometrical frustration the leading mechanism to increase the kinks' concentration. As expected in this regime, a maximally geometric frustrated system should exhibit the maximum of the mobility. According to the literature, the maximal geometric frustration occurs when the commensuration is equal to the golden mean, i.e., $\zeta = 2/(\sqrt{5}+1)$.[58] This fact explains why in Figs. 5 and 6 the mobility at intermediate values or substrate potential has a maximum at a value close to the golden mean. In such a condition, a further increase of the substrate potential, or analogously a decrease of temperature, produces a sort of solidification of the dense system of strongly interacting kinks, which reflects in a sudden decrease of the mobility exactly at the same commensurations where originally the mobility used to have a maximum.

V. CONCLUSIONS

In this work, we used a generalized Frenkel-Kontorova model to study the mobility of water confined in a carbon nanotube with very small radius. In this highly confined regime,

the water molecules form an almost one-dimensional network of highly oriented particles linked by the hydrogen bond. We described such a system as a one-dimensional chain of particles interacting through a core-softened potential of two length scales.

We performed Langevin's simulations for a system of water-like particles and studied the behavior of the total friction coefficient in the low temperature regime. For all parameters adopted in this work, we observed wet friction. Our computational results show a quadratic increasing monotonic behavior of the friction coefficient as a function of corrugation, at fixed commensurations. At the same time, the friction coefficient shows a non-monotonic behavior varying commensurations at fixed amplitudes of the substrate potential. Such a result for the friction coefficient is better observed in our family of mobility versus commensuration curves, for different corrugations. These two behaviors obtained corroborate the results reached through atomistic simulations of TIP3P water confined in carbon nanotubes developed by Falk *et al.*,[18] where they concluded that the incommensurability between water and carbon nanotubes is the main result for the high flux observed in this system. Additionally, although obtained from an effective model, our results open a path for the understanding of the physical phenomenon responsible for the variety of results obtained for the water flow in CNTs.[10–18] From a computational perspective, each atomistic model of water has its own geometric parameters. These small geometric differences between the various water models result in different lengths for hydrogen bonds, for example. Therefore, different water models have different commensuration ratios with the nanotube, and as our results consistently show, even small changes in the commensuration ratio affect the mobility.

The mobility curves not only show a non-monotonic behavior of this quantity varying commensuration but also indicate the existence of different regimes depending on the amplitude of the corrugated potential. In order to qualitatively understand the computational results for the mobility, we study analytically a simplified version of our model, the driven Frenkel-Kontorova model, at finite temperatures. As a result, we obtain numerically the curves of mobility versus commensurations at fixed substrate potentials which as discussed previously show the existence of three regimes of behavior of such a quantity with variations of commensurations. These regimes can be related to the density and dynamics of the defects in our chain of particles in a scenario analogous to the one proposed by Braun *et al.*,[50,51] considering a sort of inverse relation between temperature and amplitude of the substrate potential.

In this sense, the main result of this work is the existence of a relation between the effective substrate potential with temperature, commensuration, and bare substrate potential. This relation although simple shows that even in our simplified model, there is a nontrivial and strong dependence of the effective substrate potential with the model parameters (temperature, commensuration, and substrate potential), which at the same time makes the mobility of the system strongly dependent on these quantities. This result adds one more ingredient to the discussion of the differences between studies on water flow.[10–18] As we have already discussed, the commensuration ratio certainly plays an important role for the mobility, but other parameters of the system like temperature and corrugation are relevant as well.

When we compare the analytic and the simulation results for the mobility varying commensuration, at fixed substrate potential, some similarities arise. Although it is expected that the form of the potential exerts a critical influence on the detailed form of the mobility curves, we can indeed identify in both cases a regime for small amplitudes of the potential in which we have a displacement of the maximum of the mobility from higher to lower values of the commensuration. This crossover was theoretically identified as a result of the variation in the relative population of geometric and thermal kinks. We expect the same mechanism to be responsible for the observed behavior in the generalized Frenkel-Kontorova model. Increasing the substrate potential, our model for water-like particles develops a change in the curvature of the mobility curves evident as an additional drop in the mobility at commensurations close to the golden mean. This behavior in our generalized FK model could be explained by the same mechanism that produces a drop in the mobility for the FK model, i.e., structuring of a large number of geometric induced defects in the system.

Although we are aware that further studies are needed to confirm the proposed mechanisms as responsible for the observed features of the mobility curves, in the generalize FK model, we expect that the present work motivates and sheds some light on the physics involving the transport process of water particles in extreme confinement conditions.

Finally, we would like that this work motivates the use of the various experimental and theoretical methods developed originally for the study of sliding friction in nanoscale, to understand the water behavior in nano-confined conditions.

SUPPLEMENTARY MATERIAL

See supplementary material for the complete description of $V(x_{ij})$ and $U(x_i)$ determination.

ACKNOWLEDGMENTS

This work is partially supported by Brazilian agency CNPq (Project No. 151262/2009-8), CAPES (Project No. 23038002179/2012-50), Universidade Federal do Rio Grande do Sul, and Universidade Federal de Santa Catarina.

[1] T. I. S. Iijima, Nature **363**, 603 (1993).
[2] A. I. Kolesnikov, J.-M. Zanotti, C.-K. Loong, P. Thiyagarajan, A. P. Moravsky, R. O. Loutfy, and C. J. Burnham, Phys. Rev. Lett. **93**, 035503 (2004).
[3] N. Naguib, H. Ye, Y. Gogotsi, A. G. Yazicioglu, C. M. Megaridis, and M. Yoshimura, Nano Lett. **4**, 2237 (2004).
[4] W. Wu, S. Wieckowski, G. Pastorin, M. Benincasa, C. Klumpp, J.-P. Briand, R. Gennaro, M. Prato, and A. Bianco, Angew. Chem., Int. Ed. **44**, 6358 (2005).
[5] A. Barroug and M. J. Glimcher, J. Orthop. Res. **20**, 274 (2002).
[6] P. Pai, K. Nair, S. Jamade, R. Shah, V. Ekshinge, and N. Jadhav, Curr. Pharm. Res. J. **1**, 11 (2006).
[7] D. Pantarotto, C. D. Partidos, J. Hoebeke, F. Brown, E. Kramer, J.-P. Briand, S. Muller, M. Prato, and A. Bianco, Chem. Biol. **10**, 961 (2003).
[8] N. W. S. Kam, M. O'Connell, J. A. Wisdom, and H. Dai, Proc. Natl. Acad. Sci. U. S. A. **102**, 11600 (2005).

[9]R. G. Ding, G. Q. Lu, Z. F. Yan, and M. A. Wilson, J. Nanosci. Nanotechnol. **1**, 7 (2001).
[10]J. K. Holt, H. G. Park, Y. Wang, M. Stadermann, A. B. Artyukhin, C. P. Grigoropoulos, A. Noy, and O. Bakajin, Science **312**, 1034 (2006).
[11]M. Majumder, N. Chopra, R. Andrews, and B. J. Hinds, Nature **438**, 44 (2005).
[12]X. Qin, Q. Yuan, Y. Zhao, S. Xie, and Z. Liu, Nano Lett. **11**, 2173 (2011).
[13]J. P. N. G. Hummer and J. C. Rasaiah, Nature **414**, 188 (2001).
[14]A. Kalra, S. Garde, and G. Hummer, Proc. Natl. Acad. Sci. U. S. A. **100**, 10175 (2003).
[15]J. A. Thomas and A. J. H. McGaughey, Nano Lett. **8**, 2788 (2008).
[16]J. A. Thomas and A. J. H. McGaughey, Phys. Rev. Lett. **102**, 184502 (2009).
[17]M. H. Kohler, J. R. Bordin, L. B. da Silva, and M. C. Barbosa, Phys. Chem. Chem. Phys. **19**, 12921 (2017).
[18]K. Falk, F. Sedlmeier, L. Joly, R. R. Netz, and L. Bocquet, Nano Lett. **10**, 4067 (2010).
[19]C. Vega and J. L. F. Abascal, Phys. Chem. Chem. Phys. **13**, 19663 (2011).
[20]P. Mark and L. Nilsson, J. Phys. Chem. A **105**, 9954 (2001).
[21]L. Xu, N. Giovambattista, S. V. Buldyrev, P. G. Debenedetti, and H. E. Stanley, J. Chem. Phys. **134**, 064507 (2011).
[22]A. B. de Oliveira, P. A. Netz, T. Colla, and M. C. Barbosa, J. Chem. Phys. **124**, 084505 (2006).
[23]S. Buldyrev, G. Franzese, N. Giovambattista, G. Malescio, M. Sadr-Lahijany, A. Scala, A. Skibinsky, and H. Stanley, Physica A **304**, 23 (2002).
[24]N. M. Barraz, E. Salcedo, and M. C. Barbosa, J. Chem. Phys. **131**, 094504 (2009).
[25]A. B. de Oliveira, P. A. Netz, T. Colla, and M. C. Barbosa, J. Chem. Phys. **125**, 124503 (2006).
[26]A. Alexiadis and S. Kassinos, Chem. Eng. Sci. **63**, 2793 (2008).
[27]R. J. Mashl, S. Joseph, N. R. Aluru, and E. Jakobsson, Nano Lett. **3**, 589 (2003).
[28]J. Wang, Y. Zhu, J. Zhou, and X.-H. Lu, Phys. Chem. Chem. Phys. **6**, 829 (2004).
[29]S. Guo, E. R. Meshot, T. Kuykendall, S. Cabrini, and F. Fornasiero, Adv. Mater. **27**, 5726 (2015).
[30]E. Secchi, S. Marbach, A. Niguès, D. Stein, A. Siria, and L. Bocquet, Nature **537**, 210 (2016).
[31]C. M. Mate, G. M. McClelland, R. Erlandsson, and S. Chiang, Phys. Rev. Lett. **59**, 1942 (1987).
[32]M. L. Gee, P. M. McGuiggan, J. N. Israelachvili, and A. M. Homola, J. Chem. Phys. **93**, 1895 (1990).
[33]S. Granick, Science **253**, 1374 (1991).
[34]J. Krim, D. H. Solina, and R. Chiarello, Phys. Rev. Lett. **66**, 181 (1991).
[35]E. T. Watts, J. Krim, and A. Widom, Phys. Rev. B **41**, 3466 (1990).
[36]A. Dayo, W. Alnasrallah, and J. Krim, Phys. Rev. Lett. **80**, 1690 (1998).
[37]M. Cieplak, E. D. Smith, and M. O. Robbins, Science **265**, 1209 (1994).
[38]E. D. Smith, M. O. Robbins, and M. Cieplak, Phys. Rev. B **54**, 8252 (1996).
[39]B. Persson and A. Nitzan, Surf. Sci. **367**, 261 (1996).
[40]M. S. Tomassone, J. B. Sokoloff, A. Widom, and J. Krim, Phys. Rev. Lett. **79**, 4798 (1997).
[41]W. L. Schaich and J. Harris, J. Phys. F: Met. Phys. **11**, 65 (1981).
[42]F. Sols and F. Flores, Solid State Commun. **42**, 687 (1982).
[43]B. N. J. Persson, Phys. Rev. B **44**, 3277 (1991).
[44]B. N. J. Persson and A. I. Volokitin, J. Chem. Phys. **103**, 8679 (1995).
[45]J. B. Sokoloff, Phys. Rev. B **52**, 5318 (1995).
[46]A. Liebsch, Phys. Rev. B **55**, 13263 (1997).
[47]I. Altfeder and J. Krim, J. Appl. Phys. **111**, 094916 (2012).
[48]A. Liebsch, S. Gonçalves, and M. Kiwi, Phys. Rev. B **60**, 5034 (1999).
[49]E. S. Torres, S. Goncalves, C. Scherer, and M. Kiwi, Phys. Rev. **73**, 035434 (2006).
[50]O. M. Braun and Y. S. Kivshar, Phys. Rev. B **50**, 13388 (1994).
[51]O. M. Braun, T. Dauxois, M. V. Paliy, and M. Peyrard, Phys. Rev. B **54**, 321 (1996).
[52]E. Salcedo, N. M. Barraz, and M. C. Barbosa, J. Chem. Phys. **138**, 164502 (2013).
[53]M. P. Allen, Mol. Phys. **47**, 599 (1982).
[54]J. Krim and A. Widom, Phys. Rev. B **38**, 12184 (1988).
[55]B. Bhushan, J. N. Israelachvili, and U. Landman, Nature **374**, 607 (1995).
[56]J.-L. Barrat and L. Bocquet, Faraday Discuss. **112**, 119 (1999).
[57]T. Strunz and F.-J. Elmer, Phys. Rev. E **58**, 1601 (1998).
[58]M. Peyrard and S. Aubry, J. Phys. C: Solid State Phys. **16**, 1593 (1983).